Point defects on the (110) surfaces of InP, InAs, and InSb: A comparison with bulk

A. Höglund,[1] C. W. M. Castleton,[2,3] M. Göthelid,[2] B. Johansson,[1,4] and S. Mirbt[1]
[1]*Condensed Matter Theory Group, Department of Physics, Uppsala University, Box 530, SE-751 21 Uppsala, Sweden*
[2]*Material och Halvledarfysik, IMIT, KTH, Electrum 229, SE-16440 Kista, Sweden*
[3]*Department of Materials Chemistry, Box 538, SE-751 21, Uppsala, Sweden*
[4]*Applied Materials Physics, Department of Materials Science and Engineering, Royal Institute of Technology, SE-100 44 Stockholm, Sweden*

(Received 12 December 2005; revised manuscript received 9 May 2006; published 29 August 2006)

The basic properties of point defects, such as local geometries, positions of charge-transfer levels, and formation energies, have been calculated using density-functional theory, both in the bulk and on the (110) surface of InP, InAs, and InSb. Based on these results we discuss the electronic properties of bulk and surface defects, defect segregation, and compensation. In comparing the relative stability of the surface and bulk defects, it is found that the native defects generally have higher formation energies in the bulk. From this it can be concluded that at equilibrium there is a considerably larger fraction of defects at the surface and under nonequilibrium conditions defects are expected to segregate to the surface, given sufficient time. In most cases the charge state of a defect changes upon segregation, altering the charge-carrier concentrations. The photothresholds are also calculated for the three semiconductors and are found to be in good agreement with experimental data.

DOI: 10.1103/PhysRevB.74.075332 PACS number(s): 68.35.Dv, 61.72.−y, 61.72.Ji, 71.55.−i

I. INTRODUCTION

Native point defects in Si and GaAs bulk have been studied intensively for many years because of their strong influence on the electronic properties of these materials as well as their role as nucleation centers for unwanted oxide growth and stacking faults. For Si a very high level of perfection has been achieved, with vanishingly low defect densities.[1] In compound semiconductors, the problem is more complex since, in addition to vacancies and interstitial defects, antisite defects may also occur. The relative concentrations of the defects as well as their charge states determine the Fermi level position. In addition, the interaction of defects with dopants and unwanted impurities may alter the relative stability.[2] Most experimental studies on III-V compound surfaces have been done on GaAs and InP and in particular for the cleavage surfaces.[2,3] One reason for this is the fact that cleaving can produce defect free surfaces; whereas other crystal orientations require sputter-anneal cleaning that itself induces defects. In addition to being cleavage induced or sputter induced,[2] surface defects may also be generated by segregation of bulk defects to the surface. The distribution of bulk defects has been studied directly with cross-sectional scanning tunneling microscopy (STM) where bulk defects were exposed by cleaving the crystal.[3] Surface vacancies, in particular anion vacancies, are readily produced by evaporation of surface atoms. On GaAs(110) and InP(110) this even occurs at room temperature, although the concentration never exceeds 0.1%. These vacancies have been determined to be positively charged in *p*-type material from the voltage dependence of STM images.[4,5] Similarly, on the *n*-type InSb(110) surface it has been found that Sb vacancies are the most common type of defect.[6] On S-doped (*n*-type) InAs(110) microscopy studies have shown that the most common defects are S atoms and As vacancies,[7,8] while a third type of defect was suggested to be In vacancies.[8] The current understanding of point defects at compound semiconductor surfaces is nicely reviewed by Ebert.[9] The electronic structure and atomic geometry of anion vacancies have been studied theoretically on (110) surfaces of InP, InAs, and InSb.[5,10,11] It was shown that the charge-transfer levels are located in the center of the band gap for InP and InAs whereas in InSb the −1 charge state was stable over the whole band gap. A study of the basic properties of point defects at the (110) surface of GaAs employing density-functional theory has been done by Schwarz *et al.*[12] Previous studies of native defects in bulk InP, InAs, and InSb using *ab initio* techniques can be found in Refs. 13–19. Here, we present a comparative study of all the native bulk and surface defects in three compound semiconductors that share the same cation, InP, InAs, and InSb. This study treats all six systems using exactly the same methods and the same level of accuracy. Hence this is the first study which can try to make direct comparisons between these three materials and between the bulk and surface of each material, drawing definite conclusions about segregation and anion dependence of In-(V) semiconductors. The types of surface defects considered are shown in Fig. 1. The emphasis is put on the relative defect stability between the surface and bulk. In agreement with expectations we show that there is a tendency for the formation energy of native defects to be lower at the surface. Native point defects are therefore, in general, more stable at the surface than in bulk and are expected to segregate to the surface after sufficient time.

In Sec. II we will outline the details of the method used and in Sec. III we apply this and calculate properties of the three defect free materials. Section IV discusses the differences between the bulk and surface calculations and how to make a good comparison between the two. In Sec. V the results are presented and in Sec. VI we conclude.

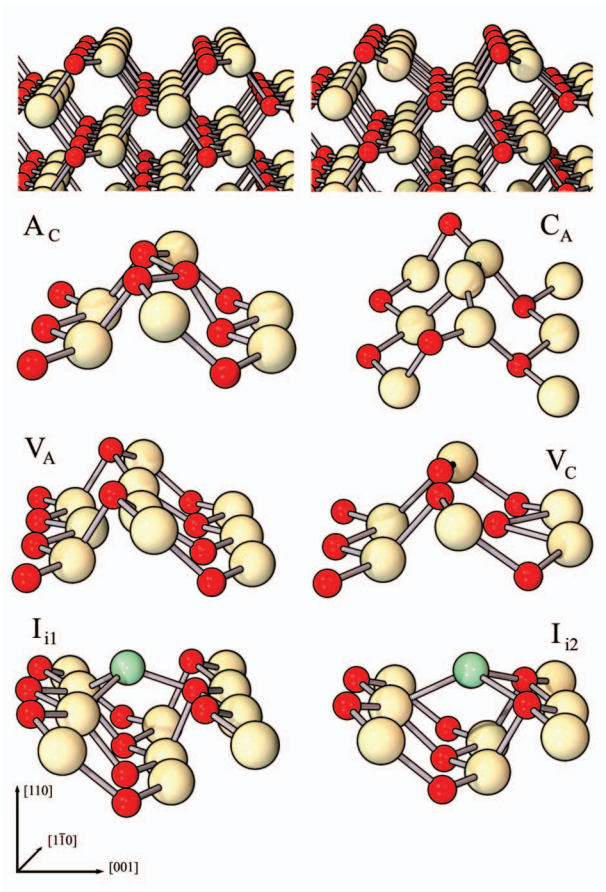

FIG. 1. (Color online) Structures of point defects on the (110) surface. Small dark atoms (red online) indicate anions, large light atoms (yellow online) indicate cations and the intermediate atoms (green online) indicate interstitial positions. First row: the defect-free surface, without (left) and with (right) reconfiguration. Second row: anion antisite A_C and cation antisite C_A. Third row: anion vacancy V_A and cation vacancy V_C. Fourth row: Interstitial positions I_{i1} and I_{i2}.

II. COMPUTATIONAL DETAILS

We use plane-wave *ab initio* density-functional theory[23] within the local-density approximation (LDA) together with ultrasoft pseudopotentials[24,25] using the VASP code.[26] Exchange and correlation potentials are described by the functional of Ceperley and Alder as parametrized by Perdew and Zunger.[27] The 4*d* electrons of the indium atom are treated as core electrons. For charged defects, a uniform compensating background is incorporated to maintain the charge neutrality of the supercell.[28] A plane-wave cutoff of 240 eV is used for all calculations, which is sufficient to reproduce surface properties.[10,29] (The exception is bulk InP, where the same level of accuracy was previously[30] found with a cutoff of 200 eV.)

For the surface defect calculations we model the (110) surface by a periodically repeated slab geometry.[31] Our supercell contains seven atomic layers with a surface unit cell of (2×4) and separated by a vacuum region of 10 Å thickness,[32] while the bottom surface layer is passivated by pseudohydrogens[33] (see Fig. 2). The top four atomic layers

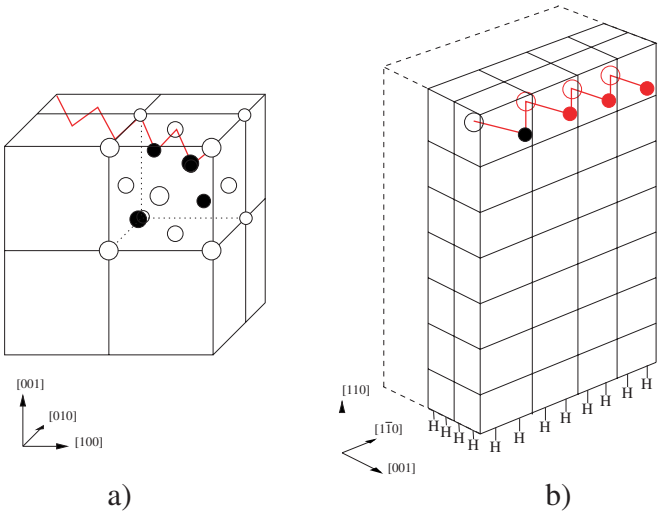

FIG. 2. (Color online) Schematic illustrations of the supercells used: (a) shows the bulk and (b) the 110 surface. (Twice the surface cell is indicated by dashed lines.)

are allowed to relax until the forces are less than 0.01 eV/Å. After testing the convergence of total energy and structure, we use a Monkhorst-Pack[34] grid of $2\times2\times2$ k points to sample the Brillouin zone with a smearing of $\delta=0.05$ eV.

For the bulk defect calculations we used a simple cubic supercell of 64 atoms, i.e., a $2\times2\times2$ repetition of eight atom unit cells. No restrictions are placed upon the symmetry of relaxations, but we do not allow atoms located on the boundary of the cell to relax. A Monkhorst-Pack $4\times4\times4$ k-point grid was used.[30]

The method used is expected to give errors in absolute values on the order of ~0.5 eV, arising primarily from the relatively small size of the supercells and from the LDA itself. However, the accuracy of the comparisons, which is the main issue in this paper, are expected to be considerably better. This is because the materials, supercells, and defects are very similar, so the errors in the various formation energies and transfer levels will also be similar. This leads to significant cancelation of errors when comparing the same (or equivalent) defects between different materials or between the surface and the bulk.

III. DEFECT-FREE RESULTS

Before performing calculations involving defects we first optimize the lattice constants subject to the LDA. The results for this and the calculated band gaps are shown and compared to experimental data in Table I.

A. Surface reconfiguration

The reconfiguration of the ideal defect-free surface has little effect on the bond lengths, as shown in the top row of Fig. 1. In the top layer the In-As bond distance decreases by only 0.02 Å from the bulk distance of 2.60 Å, compared to reductions of 0.03 Å from 2.49 Å in InP and 0.01 Å from 2.78 Å in InSb. This is in accordance with experimental observations, where it has been found that surface reconfigura-

TABLE I. Calculated lattice constant a [Å], photothreshold Φ [eV], and the calculated (LDA) band gap of the supercell E_g [eV], compared with respective experimental (Expt.) values taken from Refs. 20–22.

	a	$a^{Expt.}$	Φ	$\Phi^{Expt.}$	$E_g^{Surface}$	E_g^{Bulk}	$E_g^{Expt.}$
InP	5.828	5.869	5.69	5.69	1.106	0.660	1.424
InAs	6.013	6.058	5.27	5.31	0.539	0.000	0.417
InSb	6.430	6.479	4.95	4.77	0.528	0.000	0.235

tion alters the bond angles but leaves the bond lengths essentially unchanged.[35] The surfaces are reconfigured such that the anions are located farther away from the surface than the cations. The anions have a completely filled dangling bond pointing outwards from the surface. The cations have three valence electrons, now distributed on three bonds and rehybridized to give an almost planar sp^2-like bonding structure.

B. Photothreshold

The Photothreshold Φ,

$$\Phi = E_\infty - \mathrm{VBM}, \tag{1}$$

is defined as the energy difference between the vacuum level E_∞, and the valence-band maximum VBM. We determined E_∞ by searching for the maximal local potential within the vacuum region of the surface slab and the VBM was determined at the Gamma point. The results are listed in Table I. The experimentally determined photothreshold agrees rather well with the calculated one. This confirms that the VBM is well determined in spite of the LDA error.

IV. PROBLEMS OF COMPARING BULK AND SURFACE DEFECTS

A. Defect segregation and formation energy

Consider an infinite crystal where a fraction k of the lattice sites are defect sites. If a finite piece of this crystal is cut out at $t=0$ the fraction of surface defects will be the same as in bulk, $k_S/k_B=1$. If, after a period of time, the fraction of surface defects is larger than that in bulk the defect is said to undergo surface segregation. The fraction of defect sites can be derived from the Gibbs free energy of the system,[36]

$$k = \frac{n}{N} = e^{-\varepsilon^{form}/k_B T} e^{S^{form}/k_B}, \tag{2}$$

where n is the number of defect sites, N is the number of possible defect sites in the lattice, ε^{form} is the formation energy of the defect, and S^{form} is the formation entropy, i.e., all entropy contributions other than the configurational entropy. The ratio k_S/k_B can then be expressed as

$$\frac{k_S}{k_B} = e^{(\varepsilon_B^{form} - \varepsilon_S^{form})/k_B T} e^{(S_S^{form} - S_B^{form})/k_B}. \tag{3}$$

The vibrational term constitutes the main part of the formation entropy[37,38] and it has been shown that the difference in the vibrational entropy between the surface and bulk material, at for example the (001) Fe and MgO surfaces, is, in fact, negligible in comparison to the formation energy.[39,40] The second factor in Eq. (3) is therefore approximately equal to 1. The formation energy difference, which will be referred to as the segregation energy, will therefore dictate whether the ratio in Eq. (3) will be larger or smaller than 1, that is, if a defect will segregate to the surface or diffuse into the material.

The formation energy ε^{form} of a point defect in charge state q depends on the anion (cation) chemical potential μ_A (μ_C) and the Fermi level ϵ_F (measured from the valence-band maximum E_v):

$$\varepsilon^{form} = E_{def}^{Tot} - E_{ideal}^{Tot} - n_A \mu_A - n_C \mu_C + q(E_v + \epsilon_F), \tag{4}$$

where E_{def}^{Tot} and E_{ideal}^{Tot} are the total energy of the supercell with and without the defect (See Fig. 3).[29] The defect is formed by adding $n_{A(C)}$ anion (cation) atoms. The chemical potentials of the cations and the anions are restricted to be lower than or equal to the corresponding pure bulk values and also such that their sum is equal to the chemical potential of the III-V semiconductor. Because of these conditions only one of them is an independent parameter. We choose this to be the anion chemical potential. In InAs for example, the value of the anion chemical potential is restricted to the interval $\mu_{InAs} - \mu_{In}^{Bulk} \leq \mu_{As} \leq \mu_{As}^{Bulk}$, where the lower limit is re-

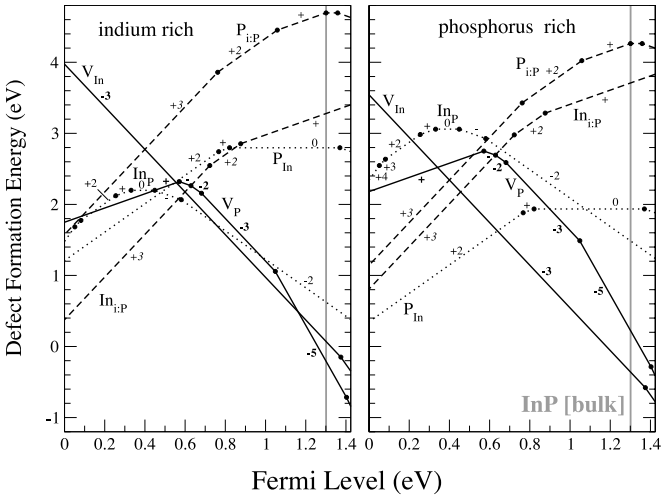

FIG. 3. Formation energy of the native point defects in bulk InP as a function of the Fermi level under In rich conditions with chemical potential $\mu_P=-6.46$ eV and under P rich conditions with $\mu_P=-6.03$ eV. Solid, dashed, and dotted lines denote vacancies, interstitials, and antisites, respectively. (Transitions above the thin vertical gray line are not reliable since they correspond to occupancies of the Kohn-Sham conduction-band states.)

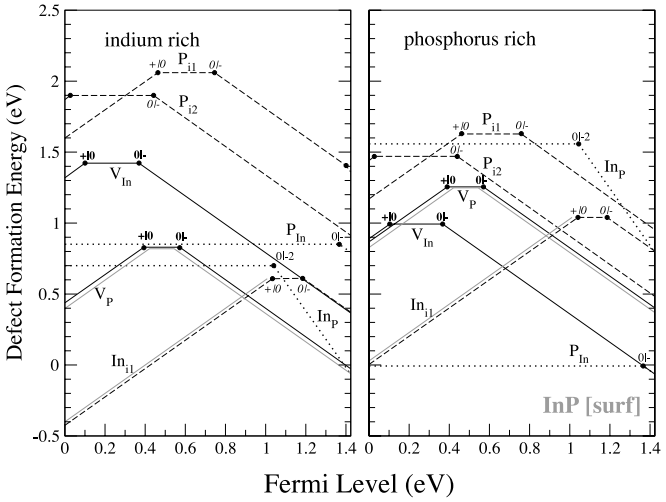

FIG. 4. Formation energy of the native point defects on the InP(110) surface as a function of the Fermi level under In rich conditions with chemical potential μ_P=−6.46 eV and under P rich conditions with μ_P=−6.03 eV. Solid, dashed, and dotted lines denote vacancies, interstitials and antisites, respectively. Thin gray lines indicate calculations performed with twice the surface cell according to Fig. 2.

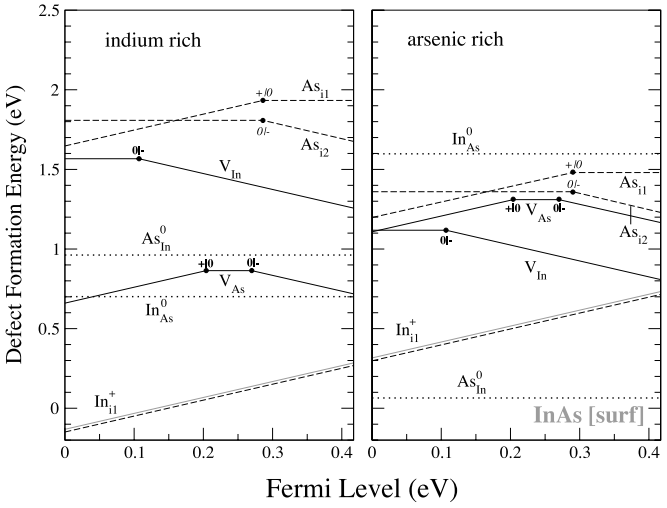

FIG. 6. Formation energy of the native point defects on the InAs(110) surface as a function of the Fermi level under In rich conditions with chemical potential μ_{As}=−5.85 eV and under As rich conditions with μ_{As}=−5.40 eV. Solid, dashed, and dotted lines denote vacancies, interstitials, and antisites, respectively. Thin gray lines indicate calculations performed with twice the surface cell according to Fig. 2.

ferred to as the In rich case and the upper limit as the As rich case. We use μ_P^{Bulk}=−6.027 eV, μ_{As}^{Bulk}=−5.404 eV, μ_{Sb}^{Bulk}=−4.823 eV, and μ_{In}^{Bulk}=−3.269 eV.

Our calculated formation energies are presented in Figs. 4–7 in the following order: InP bulk, InP surface, InAs bulk, InAs surface, InSb and bulk, InSb surface.

B. Supercell

The defect formation energy depends on the size of the supercell used, because of the interaction of the defect with its periodic images. For example, the dependence can be as strong as for the $In_{i:P}^{+3}$ interstitial in InP, where the formation energy changes from 0.6 eV in the 64 atom supercell to 1.3 eV in the 512 atom supercell to the extrapolated value of 1.9 eV in the infinite cell.[41] (The corresponding change for the In_P^0 is 3.0, 3.2, and 3.9 eV, so the dependence can be significant even for neutral defects.[42]) A comparison between surface and bulk defect formation energies is therefore difficult in general. We have chosen the bulk supercell which most closely resembles the surface supercell in terms of defect-defect image interaction. The surface supercell is

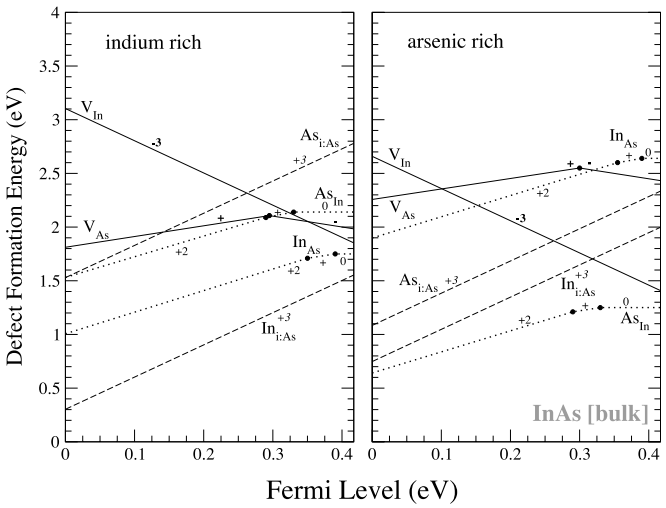

FIG. 5. Formation energy of the native point defects in bulk InAs as a function of the Fermi level under In rich conditions with chemical potential μ_{As}=−5.85 eV and under As rich conditions with μ_{As}=−5.40 eV. Solid, dashed, and dotted lines denote vacancies, interstitials, and antisites, respectively.

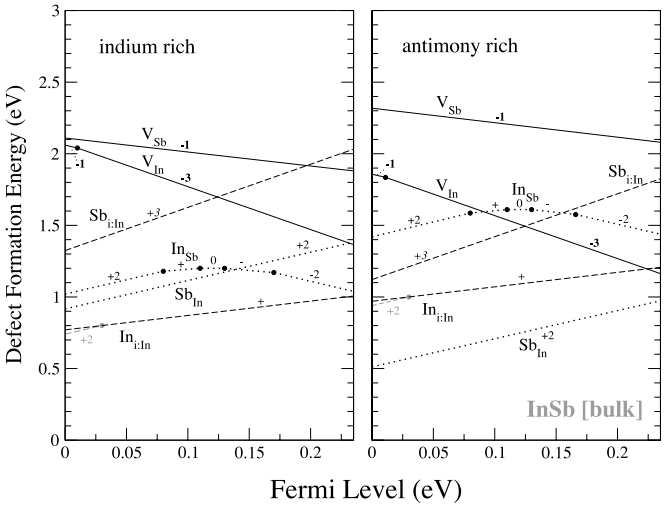

FIG. 7. Formation energy of the native point defects in bulk InSb as a function of the Fermi level under In rich conditions with chemical potential μ_{Sb}=−5.03 eV and under Sb rich conditions with μ_{Sb}=−4.82 eV. Solid, dashed, and dotted lines denote vacancies, interstitials, and antisites, respectively.

(2×4), i.e., a two-atom unit cell is repeated two (four) times in the [001] ($[1\bar{1}0]$) direction to produce a supercell containing 112 atoms in total (see Fig. 2). The defect related bands along the [001] direction are rather flat, because there are no surface bonds in the [001] direction.[10] Along the $[1\bar{1}0]$ direction the defect bands show dispersion and the formation energy depends on the number of repetitions of the single unit cell along this direction.[11] The most convenient orientation for the bulk unit cell is rotated relative to the (110) surface cell, with an eight-atom simple cubic cell along the [001], [010], and [100] directions. A $2\times2\times2$ repetition of this unit gives the same defect-defect image distances along the $[1\bar{1}0]$ bonding directions as found at the surface. The 64-atom bulk supercell thus best resembles the defect-defect interaction of the 2×4 surface supercell in terms of wave-function overlap. The Coulombic defect interaction, on the other hand, is mainly just distance dependent. In this respect twice the surface supercell in the [001] direction (as indicated in Fig. 2) would better correspond to the 64-atom bulk supercell. We have checked the scale of the additional error introduced by using the 2×4 surface cell by repeating the calculations for four of the most stable defects in this larger supercell. We find that this only leads to minor corrections, as shown by the thin gray lines in Figs. 4, 6, and 8, and does not alter the conclusions of this work.

In order to calculate comparable defect formation energies, the electrostatic potentials of the defect-free bulk and the surface have been aligned to assure a common zero energy. This was done by adding the difference of the average potential in the surface cell in a region far from the surface and the average bulk potential to the surface valence-band maximum E_v.

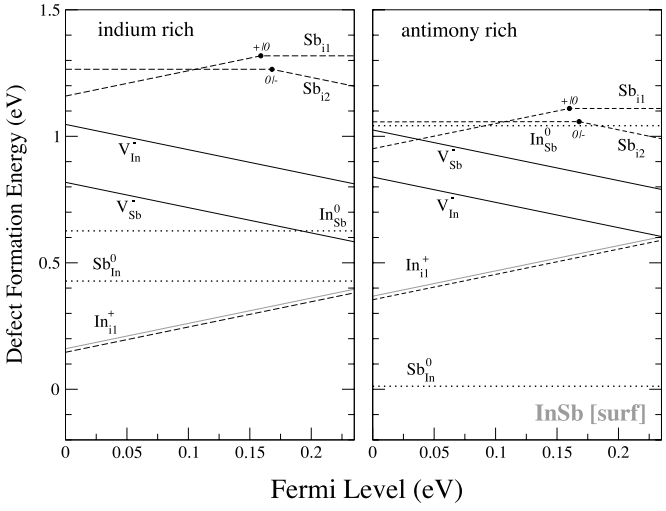

FIG. 8. Formation energy of the native point defects on the InSb(110) surface as a function of the Fermi level under In rich conditions with chemical potential $\mu_{Sb}=-5.03$ eV and under Sb rich conditions with $\mu_{Sb}=-4.82$ eV. Solid, dashed, and dotted lines denote vacancies, interstitials and antisites, respectively. Thin gray lines indicate calculations performed with twice the surface cell according to Fig. 2.

C. Band gap

Another problem is the band gap. In the expression for the defect formation energy, the Fermi energy can vary from the valence-band maximum up to the conduction-band minimum. The size of the band gap thus enters indirectly into Eq. (4). The LDA band gap differs between a supercell containing a surface (thin film) and bulk, as tabulated in Table I. This difference is explained by an artificial quantization imposed by the periodically repeated thin film.[43] For bulk InAs and bulk InSb the band gap calculated within LDA is nonexistent. Therefore the experimental band gaps are used for the calculation of the defect formation energy for all three materials, both in the bulk and at the surface. This is justified since the band gap is only zero (or close to zero) at the Γ point, at other k points and especially at the special k points used, the difference between the highest occupied and lowest unoccupied state is greater than the experimental band gap. This means that, at least in principle, we do not expect occupation of conduction-band Kohn-Sham states. We have confirmed that this indeed holds for the results presented here, by checking that the defects had neither electrons in the conduction band nor holes in the valence band. This was done by plotting the charge distributions of the defect states, making sure they are localized and centered at the defect site. This is true for all defects except $P_{i:P}^{0,-1}$, V_{In}^{-4}, P_{In}^{-1}, and V_P^{-6} in bulk InP and $In_{i:In}^{+2}$ in bulk InSb. This implies that charge transitions within 0.1 eV from the conduction-band minimum (CBM) in bulk InP cannot be treated as reliable results (above the vertical thin gray line in Fig. 3). However, although $In_{i:In}^{+2}$ results in a delocalized hole occupying the valence band (therefore it is excluded and only indicated in gray in Fig. 7), the -1 charge state of V_{In} is perfectly localized even though it is closer to the VBM.

V. RESULTS

A. Self-doping

In Figs. 4, 6, and 8 we show the defect formation energies of the native defects at the (110) surfaces of InP, InAs, and InSb, in the order of increasing lattice constant, and in Figs. 3, 5, and 7 those of the native defects in the corresponding bulk materials. It is known that nominally undoped InAs is n-type doped due to native defects. Our calculated results confirm that InAs becomes n-type doped. From Figs. 6 and 5 it is seen that the In interstitial has the overall lowest defect formation energy under In rich conditions. The In_i is positively charged over the entire band gap, with a +3 (+1) charge state in the bulk (surface). Each interstitial will therefore, in the absence of acceptors, donate three (one) electrons to the conduction band and set the Fermi level equal to the conduction-band minimum. In the arsenic rich bulk case things are complicated somewhat since here As_{In} will be the most common donor. Also acceptors are present, V_{In}^{-3} being the most common, so the electrons will instead populate them and the Fermi energy will be determined by the equilibrium between native acceptors and native donors. The Fermi level will be pinned at the intersection of the formation energies of the acceptor and the donor, that is, 0.09 eV

TABLE II. Segregation energies under *p*-type, semi-insulating, and *n*-type conditions. Segregation energies are independent of growth conditions.

InP	V_P	V_{In}	P_i	In_i	P_{In}	In_P
p-type	1.4	2.7	0.0	0.8	0.4	0.8
semi-ins.	1.3	0.7	2.0	2.3	1.8	1.1
n-type	−0.8	−0.6	3.8	2.9	2.0	0.4
InAs	V_{As}	V_{In}	As_i	In_i	As_{In}	In_{As}
p-type	1.1	1.5	−0.1	0.4	0.6	0.3
semi-ins.	1.1	1.0	0.4	0.9	0.9	0.7
n-type	1.3	0.3	1.1	1.2	1.2	1.1
InSb	V_{Sb}	V_{In}	Sb_i	In_i	Sb_{In}	In_{Sb}
p-type	1.3	1.0	0.1	0.6	0.5	0.4
semi-ins.	1.3	0.8	0.4	0.6	0.7	0.6
n-type	1.3	0.6	0.8	0.6	1.0	0.4

below the conduction-band minimum, since the neutral state of As_{In} does not contribute to the Fermi-level pinning. Applying the same arguments to the surface it is seen that the Fermi level is pinned at the conduction-band minimum for both the indium rich surface and for the arsenic rich surface. From this it is concluded that InAs, as expected, will be intrinsically *n* type.

Following the same arguments as for InAs we find that both the InSb surface and bulk is expected to be intrinsically *n* type, see Figs. 7 (Fig. 8). InP is predicted to be intrinsically semi-insulating since for the bulk (surface) the Fermi level is pinned at about 0.6 eV (0.7–0.9 eV) above the valence band maximum, as seen in Fig. 3 (Fig. 4).

B. Surface segregation

In Figs. 3–8 we show the calculated defect formation energies for the native point defects at the (110) surfaces and in the bulk. A typical bulk defect has four nearest neighbors, whereas a typical (110) surface defect has three nearest neighbors. Moreover, at the surface the defect can interact with neighboring dangling bonds helping to locally increase the surface stability. This lower coordination and interaction with dangling bonds explains why defects generally have lower formation energies at the surface than in the bulk.[12] Indeed, we find that all native point defects have lower formation energies at the surface than in the bulk, with the exception of the two types of vacancies in *n*-type InP and the As interstitial in *p*-type InAs. The point defects have on the order of 1 eV lower formation energies at the surface. The segregation energies are summarized in Table II. Since we do not discuss any energy barriers it is not possible to judge which native defects will segregate. However, assuming that the native point defects are not all permanently trapped in their bulk positions, the lower surface formation energies suggest that the native defects are more stable at the surface and will therefore segregate, increasing the defect concentration at the surface and lowering it in the bulk after some sufficient time. In other words, leaving kinetic issues aside, the presence of the surface in principle depletes the bulk of native point defects.

The segregation process for the antisites is more complicated since they, unlike vacancies and interstitials, cannot migrate on their own and therefore the migration mechanism must be taken into account. A discussion of this will follow in the antisite section.

In the following we compare in detail the surface formation energies with the bulk formation energies for the six different types of defects.

1. Anion vacancy

The bulk anion vacancy shows the well-known negative-*U* behavior.[44] In InP and InAs the charge state changes directly from +1 to −1 and in InP there is also an additional negative-*U* transition from −3 to −5. In InSb the vacancy is always in a −1 charge state due to the narrow band gap.

The energy cost of removing an electron from the partially occupied In dangling bonds increases with increasing localization, i.e., the more localized the electrons, the more tightly bound they are. This is reflected in the position of the (+|−) negative-*U* transition, the higher it is in the band gap the easier it is for the defect to give up electrons and form positive charge states. Assuming a larger lattice constant and hence a smaller overlap of wave functions leads to stronger localization, a (+|−) transition higher in the band gap would correspond to a smaller lattice constant. For bulk InP with the smallest lattice constant, the (+|−) transition is located 0.6 eV above the VBM (Fig. 3). For bulk InAs, with the intermediate lattice constant, the (+|−) negative-*U* level is found at about 0.3 eV above the VBM (Fig. 5) and for InSb, with the largest lattice constant, it has disappeared into the valence band such that only the singly negative charge state is stable. The same tendency is also seen for the surfaces. At the surface the relaxation energies are approximately half of

their bulk counterparts[10] and therefore the negative-U behavior, which is a relaxation effect, is absent. Therefore there is a normal ordering of the transition levels and the charge state changes from +1 via 0 to −1. Looking instead at the $(+|0)$ transition, it is found to be located 0.4 and 0.2 eV above the VBM at the InP and InAs surface, respectively. At the InSb surface, again only the −1 charge state is stable over the entire band gap.

In order to create a vacancy, four bonds have to be broken in the bulk but only three have to be broken at the surface. The vacancies, in general, therefore have a lower energy at the surface. The P vacancy in InP under p-type (n-type) conditions gains 1.4 eV (−0.8 eV) by segregation to the surface. Similarly the As vacancy in InAs and the Sb vacancy in InSb, under p-type (n-type) conditions, gains 1.1 eV (1.3 eV) and 1.3 eV (1.3 eV) by segregation to the surface, respectively. The anion vacancy has the same charge state in bulk as at the surface for InAs and InSb under both p-type and n-type conditions. In p-type InPthe charge state does not change during segregation and under n-type conditions the anion vacancy instead gains energy by segregating into the bulk, changing its charge state from −1 to −5. Therefore the anion vacancy in InP acts as an acceptor during segregation, independent of the direction of the segregation, whereas in InAs and InSb the charge-carrier concentration is not altered.

Anion vacancies have been observed at the InP surface and the n-type surfaces of InSb and InAs. This is in agreement with our results for In-rich conditions where V_P, V_{Sb}, and V_{As} occur in high concentrations and are more stable than the cation vacancies. However, we do not always find the anion vacancies to be the most common of all native defects: the In interstitials and the antisites (In_{As} in InAs and Sb_{In} in InSb) should have higher surface concentrations according to our results. This is reasonable since the experimental surfaces were cleaved and the anion vacancies diffuse much more easily than the large In interstitials and especially the antisites, which are always dependent on other defects to occur in sufficient numbers, as discussed below.

2. Cation vacancy

At the surface the cation vacancy displays the same dependence of the transition level position on the lattice constant as described for the anion vacancy (Figs. 4, 6, and 8). The $(0|-)$ transition level is located 0.4 eV and 0.1 eV above the VBM for InP and InAs, respectively. At the InSb surface only the −1 charge state is stable over the entire band gap. In all three bulk compounds, the cation vacancy is always most stable in the −3 charge state, regardless of the Fermi-level position (with the exception of −2 in strongly p-type InSb). The In vacancy in p-type (n-type) InP, InAs, and InSb gains, respectively, 2.7 eV (−0.6 eV), 1.5 eV (0.3 eV), and 1.0 eV (0.6 eV) by segregating to the surface. Under n-type conditions, the In vacancy has a charge state of −3 in the bulk and −1 at the surface for all three materials. Therefore it acts as a donor during surface segregation in InAs and InSb but as an acceptor in InP since the segregation energy is negative. Under p-type conditions it changes from −3 to +1 and 0 in InP and InAs and from −2 to −1 in InSb, respectively, and therefore acts as a donor in all three materials.

Considering the p-type materials, the decreasing energy difference between surface and bulk positions with increasing lattice constant is mainly due to the lower bulk formation energy of the In vacancy in materials with larger lattice constants. The In vacancy will undergo the largest inward relaxation in InSb and the smallest in InP, resulting in the anion-anion distance of the nearest neighbors being closest to the covalent bonding distance for InSb. This gives an In vacancy formation energy that is smallest in InSb and largest in InP.

3. Anion interstitial

Overall, the anion interstitial has the highest formation energy among the native defects. Even under the most favorable conditions its formation energy is rarely below 1 eV. This corresponds to concentrations on the order of 10^7 cm^{-3}, which are irrelevant in the context of compensation, for example. More importantly, in all three materials, no matter whether in the bulk or at the surface, there are always other native defects acting as donors and acceptors with much smaller formation energies. These will therefore dictate the material's electronic properties and the anion interstitial will never influence either the charge-carrier concentration or the Fermi-level position.

4. Cation interstitial

At the surface of InP, InSb, and InAs the In interstitial is most stable at the "i1" position (see Fig. 1) in charge state +1, independent of the Fermi energy. The exception is n-type InP, where the charge state is 0 or −1. In bulk InP and InAs the anion surrounded tetragonal interstitial position is lowest in energy (denoted $In_{i:P}$ and $In_{i:As}$ in Figs. 3 and 5) with a charge state +3 independent of the Fermi energy in InAs and charge states +3, +2, or +1 in InP, ranging from p-type to n-type doping. In bulk InSb the cation surrounded tetragonal interstitial position is preferred instead (denoted $In_{i:In}$). Its charge state is +1 under semi-insulating and n-type conditions and +2 under p-type conditions.

Under p-type (n-type) conditions the In interstitial would gain 0.8 eV (2.9 eV) in InP, 0.4 eV (1.2 eV) in InAs, and 0.6 eV (0.6 eV) in InSb by segregating to the surface. The cation interstitial acts as an acceptor under surface segregation in InP and InAs. In InSb the cation interstitial behaves as an acceptor for p-type conditions, but in semi-insulating and n-type InSb it does not change charge state upon segregation. Since the interstitial defect is not located at an ordinary lattice site, it will always cause strain on the surrounding crystal in bulk. This is not the case at the surface, where the formation energy is therefore lower.

5. Anion antisite

For all three (InP, InAs, InSb) surfaces, the charge state of the anion antisite is neutral, independent of the Fermi energy position (except in InP where the charge state changes to −1 just below the CBM). For bulk the three materials differ. The P antisite in InP is in a +2 charge state in p-type InP and neutral in n-type InP (the transition to a negative state just below the CBM involves filling conduction-band states and will be discarded as explained above). For p-type (n-type)

conditions the formation energy of the P antisite is about 0.4 eV (2.0 eV) lower at the surface than in the bulk. The charge state of the antisite is more negative at the surface than in the bulk, 0 and +2, respectively (−1 and 0) in *p*-type (strongly *n*-type) InP.

The As antisite in bulk InAs changes its charge state from +2 at the valence-band edge via +1 to 0 at the conduction-band edge. For *p*-type (*n*-type) conditions the As antisite has about 0.6 eV (1.2 eV) lower formation energy at the surface. The Sb antisite in bulk InSb has a charge state +2 independent of the Fermi-level position. Its formation energy is 0.5 eV (1.0 eV) lower at the surface under *p*-type (*n*-type) conditions. Both the As antisite and Sb antisite have more negative charge states at the surface than in the bulk, except in *p*-type InAs where the antisite is neutral both at the surface and in the bulk.

The lower formation energies at the surface can be explained by the possibility of the bond lengths to adjust with fewer restrictions. If the nearest neighbors were put at the equilibrium distance from the anion antisite in bulk it would cause a large strain on the surrounding crystal. When the antisite is located at the surface, however, the nearest-neighbor distance can be relaxed to the equilibrium value without affecting the remaining crystal at all. Therefore the antisite could, in principle, be as low in energy as the ideal surface. This is indeed the case for anion antisites in anion rich material, where the formation energy is very close to zero for all three compounds (Figs. 4, 6, and 8).

The As antisite has three nearest neighbors, two in the top layer at a distance of 2.48 Å and one in the second layer at a distance of 2.45 Å. This is close to twice the covalent radius for As, which is $2\times1.21=2.42$ Å, indicating an almost full adjustment. Similarly in InSb (InP), the bonding distance from the antisite to the two Sb (P) nearest neighbors in the top layer is 2.85 Å (2.23 Å) and to the one in the second layer it is 2.81 Å (2.22 Å), in close agreement to twice the covalent radius of Sb (P), which is 2.82 Å (2.20 Å).

Overall, the anion antisites in InAs, InSb, and InP have roughly 0.9 eV lower formation energy at the surface than in the bulk.

6. Cation antisite

At the surface of InP, InAs, and InSb the charge state of the cation antisite is 0 independent of the Fermi energy, except in *n*-type InP where $\mathrm{In_P^{-2}}$ is more stable. For bulk InP the charge state changes between +4 and −2, for bulk InAs from +2 to 0 and for InSb between +2 and −2. Under *p*-type (*n*-type) conditions the formation energy of the In antisite is 0.8 eV (0.4 eV), 0.3 eV (1.1eV), and0.4 eV (0.4 eV) lower at the surface than in the bulk for InP, InAs, and InSb, respectively. In all three materials the cation antisite has more negative (positive) charge states at the surface than in the bulk under *p*-type (*n*-type) conditions.

The cation antisites at the surface are less energetically favorable than the anion antisites. This is because the cation antisites try to reach a planar sp^2 configuration, similar to that of the surface reconfiguration itself, but in contrast to the anion antisites, which adopt an sp^3 configuration with a dangling bond directed away from the surface. The cation antisite therefore prefers to be located in between its three nearest neighbors, which, because of the relatively large ionic radius of indium, causes a lot of strain in the surrounding surface. For all three compounds, the distance from the antisite to the two nearest neighbors in the top layer is about 2.63 Å. This is far less than twice the covalent radius of indium, which is $2\times1.50=3.00$ Å.

Comparing the surface and bulk cation antisites, the bulk has a higher formation energy since there are four strained bonds in bulk but only three at the surface. Because of the smaller lattice constants, the strain in bulk InP and InAs is larger than in InSb. The difference in energy between bulk and surface is therefore smaller for InSb.

7. Antisite segregation

The segregation of antisite defects is more complicated since we can no longer ignore the diffusion mechanism and only consider the energy of initial and end systems. An antisite might not even end up as an antisite at the surface.

The antisite can diffuse either via the *substitutional-interstitial* or the *kick-out* mechanism. Therefore one must take into account the formation energy of the interstitial and/or the vacancy. That the antisite atom might not end up as an antisite at the surface is less of a problem since any alternative configuration then has a total formation energy lower than that of the antisite and hence the segregation energy will effectively be even larger.

We will approach this complex problem by only considering those antisites that are reasonably common in the bulk ($\varepsilon^{form}<1.0$ eV). In these cases the two mechanisms mentioned above have been looked at in detail. As before, we focus on the initial and final states and do not look at barrier heights or energies of intermediate states.

In InP the relevant antisites are $\mathrm{In_P}$ in In-rich InP under *n*-type conditions and $\mathrm{P_{In}}$ in P-rich InP under *p*-type conditions. Neither of these will migrate through the kick-out mechanism since the interstitials involved (In_i for $\mathrm{P_{In}}$ and P_i for $\mathrm{In_P}$) have high formation energies which correspond to vanishingly small concentrations. Considering the substitutional-interstitial mechanism, $\mathrm{In_P}$ leaves a phosphorus vacancy behind for which it is more favorable to remain in the bulk. The In interstitial gains energy from segregating to the surface but overall, comparing the total formation energy of the reactants and products, almost no energy is gained from this process. The most likely outcome is then a recombination of the vacancy and interstitial, so little or no segregation of $\mathrm{In_P}$ is expected. For $\mathrm{P_{In}}$, on the other hand, both the resulting vacancy and interstitial will segregate to the surface. At the surface they are 2.1 eV more stable in the form of the antisite. Therefore the energy gained from the substitutional-interstitial segregation will be equal to the formation energy difference of $\mathrm{P_{In}}$ between bulk and surface, i.e., 0.4 eV.

In InAs the relevant antisites are $\mathrm{In_{As}}$ in In-rich InAs and $\mathrm{As_{In}}$ in As-rich InAs, both under *p*-type conditions. For $\mathrm{In_{As}}$ the kick-out mechanism is not possible since the As interstitial does not occur in relevant amounts. For $\mathrm{As_{In}}$ the actual kicking out of the As atom is likely to take place (0.2 eV is

gained in doing so), but the resulting As interstitial is actually slightly more stable in the bulk. Therefore the kick-out mechanism will not lead to surface segregation in InAs. Indeed, As_{In} will not segregate at all since As_i itself will not. The In antisite, on the other hand, may segregate via the substitutional-interstitial mechanism, gaining 0.3 eV in the process.

In InSb, Sb_{In} in Sb-rich material under *p*-type conditions is the most common antisite. It also occurs, but to a lesser extent, in In-rich InSb under *p*-type conditions and in Sb-rich InSb under *n*-type conditions. In *p*-type InSb the In interstitials have a relatively low formation energy such that the kick-out mechanism is possible. At the surface, the Sb interstitial is less energetically favorable than the Sb antisite plus the In interstitial in both In-rich and Sb-rich material. Therefore the final configuration is the same as the initial, an Sb antisite and an In interstitial, and comparing the formation energies in the bulk and at the surface gives an energy reduction of 1.1 eV by this kick-out mechanism. Sb_{In} is also likely to migrate through the substitutional-interstitial mechanism and at the surface Sb_{In} is always much more stable than the two migrating species, the Sb interstitial and the In vacancy. Through this Sb_{In} gains 0.5 eV (1.0 eV) by segregating to the surface in *p*-type (*n*-type) InSb. As mentioned above, the largest bulk concentration of Sb_{In} is found in Sb-rich material under *p*-type conditions so this is where the Sb antisite segregation is expected to be most important.

VI. CONCLUSIONS AND SUMMARY

We have calculated the formation energies of the native defects both in bulk and at the (110) surface of InP, InAs, and InSb. The most common defects in all three materials are found to be the cation interstitial and anion antisite defects, plus both types of vacancies in *n*-type InP. All defects are found to have a lower formation energy at the surface than in bulk, with three exceptions: the As interstitial in *p*-type InAs, which has a slightly lower formation energy in bulk, and the two types of vacancies in *n*-type InP, which have about −0.7 eV lower formation energies in bulk. Most native defects would therefore gain energy by segregating to the surface, and will do so either if the temperature is high enough to overcome the migration barriers and/or after sufficiently long time. The segregation energies are listed in Table II but it must be kept in mind that the antisite segregation is strongly dependent on the migration mechanism, as discussed in the antisite section. The listed energies are the lower bounds on the real energy gain since considering a more realistic surface with steps and kinks may lower the surface formation energies and increase the segregation energies.[45] It should be noted that in certain cases an extremely high bulk formation energy leads to a very large segregation energy but also to a vanishingly small bulk defect concentration, hence there will be no defects to segregate.

In our approach all point defects are treated as noninteracting and, for example, saturation of the defect concentration at the surface and formation of complexes will influence the final concentrations. Furthermore, we have not investigated the energy barriers or migration kinetics, so we cannot make any comments about the migration paths or the time scales, which could, of course, be immeasurably long. The conclusion that point defects are drawn to the surface because of the relatively low surface formation energy is not surprising. On the contrary, it is one of the primary reasons why annealing works to lower the concentration of intrinsic defects in semiconductors. We also find that the charge states of most defects change upon segregation, which implies that the segregation process may alter the charge carrier densities. Furthermore, the calculated photothresholds agree well with experimental data. In conclusion, it is found that the native defects in InP, InAs, and InSb in general are more stable at the surface and are therefore expected to segregate to the surface after a sufficiently long time.

[1] D. T. J. Hurle and P. Rudolph, J. Cryst. Growth **264**, 550 (2004).
[2] Ph. Ebert, Surf. Sci. Rep. **33**, 121 (1999).
[3] Ph. Ebert, Appl. Phys. A: Mater. Sci. Process. **75**, 101 (2002).
[4] Ph. Ebert, M. Heinrich, M. Simon, K. Urban, and M. G. Lagally, Phys. Rev. B **51**, 9696 (1995).
[5] Ph. Ebert, K. Urban, L. Aballe, C. H. Chen, K. Horn, G. Schwarz, J. Neugebauer, and M. Scheffler, Phys. Rev. Lett. **84**, 5816 (2000).
[6] L. J. Whitman, J. A. Stroscio, R. A. Dragoset, and R. J. Celotta, J. Vac. Sci. Technol. B **9**, 770 (1991).
[7] A. Depuydt, N. S. Maslova, V. I. Panov, V. V. Rakov, S. V. Savinov, and C. Van Haesendonck, Appl. Phys. A: Mater. Sci. Process. **66**, S171 (1998).
[8] A. Schwarz, W. Allers, U. D. Schwarz, and R. Wiesendanger, Phys. Rev. B **61**, 2837 (2000).
[9] Ph. Ebert, Curr. Opin. Solid State Mater. Sci. **5**, 211 (2001).
[10] M. C. Qian, M. Göthelid, B. Johansson, and S. Mirbt, Phys. Rev. B **66**, 155326 (2002).
[11] M. C. Qian, M. Göthelid, B. Johansson, and S. Mirbt, Phys. Rev. B **67**, 035308 (2003).
[12] G. Schwarz, J. Neugebauer, and M. Scheffler, in Proceedings of the 25th International Conference of Phys. Semicond., Osaka, 1377 (2000).
[13] R. W. Jansen, Phys. Rev. B **41**, 7666 (1990).
[14] A. P. Seitsonen, R. Virkkunen, M. J. Puska, and R. M. Nieminen, Phys. Rev. B **49**, 5253 (1994).
[15] M. Alatalo, R. M. Nieminen, M. J. Puska, A. P. Seitsonen, and R. Virkkunen, Phys. Rev. B **47**, 6381 (1993).
[16] T. M. Schmidt, R. H. Miura, A. Fazzio, and R. Mota, Phys. Rev. B **60**, 16475 (1999); Physica B **273**, 831 (1999).
[17] M. J. Caldas, J. Dabrowski, A. Fazzio, and M. Scheffler, Phys. Rev. Lett. **65**, 2046 (1990).
[18] S. Krishnamurthy and M. A. Berding, J. Appl. Phys. **90**, 848 (2001).
[19] D. N. Talwar and C. S. Ting, Phys. Rev. B **25**, 2660 (1982).
[20] I. Vurgaftman, J. R. Meyer, and L. R. Ram-Mohan, Appl. Phys.

Lett. **89**, 5815 (2001).
[21] T. E. Fischer, Phys. Rev. **142**, 142 (1966).
[22] G. W. Gobeli and F. G. Allen, Phys. Rev. **137**, A245 (1965).
[23] W. Kohn and L. J. Sham, Phys. Rev. **140**, A1133 (1965).
[24] D. Vanderbilt, Phys. Rev. B **41**, 7892 (1990).
[25] G. Kresse and J. Hafner, J. Phys.: Condens. Matter **6**, 8245 (1994).
[26] G. Kresse and J. Furthmüller, Comput. Mater. Sci. **6**, 15 (1996).
[27] J. P. Perdew and A. Zunger, Phys. Rev. B **23**, 5048 (1981).
[28] M. Leslie and M. J. Gillian, J. Phys. C **18**, 973 (1985).
[29] N. Moll, A. Kley, E. Pehlke, and M. Scheffler, Phys. Rev. B **54**, 8844 (1996).
[30] C. W. M. Castleton and S. Mirbt, Phys. Rev. B **68**, 085203 (2003).
[31] M. Schlüter, J. R. Chelikosky, S. G. Louie, and M. L. Cohen, Phys. Rev. B **12**, 4200 (1975).
[32] B. Engels, P. Richard, K. Schroeder, S. Blügel, Ph. Ebert, and K. Urban, Phys. Rev. B **58**, 7799 (1998).
[33] K. Shiraishi, J. Phys. Soc. Jpn. **59**, 3455 (1990).
[34] H. J. Monkhorst and J. D. Pack, Phys. Rev. B **13**, 5188 (1976).
[35] W. Mönch, *Semiconductor Surfaces and Interfaces*, 3rd ed. (Springer-Verlag, Berlin, 2001), and references therein.
[36] N. W. Ashcroft and N. D. Mermin, *Solid State Physics* (Brooks/Cole, Thomson Learning, 1976).
[37] P. E. Blöchl, E. Smargiassi, R. Car, D. B. Laks, W. Andreoni, and S. T. Pantelides, Phys. Rev. Lett. **70**, 2435 (1993).
[38] D. B. Laks, C. G. Van de Walle, G. F. Neumark, P. E. Blöchl, and S. T. Pantelides, Phys. Rev. B **45**, 10965 (1992).
[39] P. Masri, P. W. Tasker, J. P. Hoare, and J. H. Harding, Surf. Sci. **173**, 439 (1986).
[40] C. Uebing, Surf. Sci. **313**, 365 (1994).
[41] C. W. M. Castleton, A. Höglund, and S. Mirbt, Phys. Rev. B **73**, 035215 (2006).
[42] C. W. M. Castleton and S. Mirbt, Phys. Rev. B **70**, 195202 (2004).
[43] S. B. Zhang, Chin-Yu Yeh, and A. Zunger, Phys. Rev. B **48**, 11204 (1993).
[44] M. Alatalo, R. M. Nieminen, M. J. Puska, A. P. Seitsonen, and R. Virkkunen, Phys. Rev. B **47**, 6381 (1993).
[45] R. C. Baetzold, Phys. Rev. B **52**, 11424 (1995).